REPORT DOCUMENTATION PAGE

Form Approved
OMB No. 0704-0188

1. REPORT DATE (DD-MM-YYYY)	2. REPORT TYPE	3. DATES COVERED (From - To)
	Technical Paper	See Attached List

4. TITLE AND SUBTITLE

See Attached List

5a. CONTRACT NUMBER
N/A

5b. GRANT NUMBER
N/A

5c. PROGRAM ELEMENT NUMBER
N/A

6. AUTHOR(S)

See Attached List

5d. PROJECT NUMBER
N/A

5e. TASK NUMBER
N/A

5f. WORK UNIT NUMBER
N/A

7. PERFORMING ORGANIZATION NAME(S) AND ADDRESS(ES)
See Attached List

8. PERFORMING ORGANIZATION REPORT NUMBER
N/A

9. SPONSORING / MONITORING AGENCY NAME(S) AND ADDRESS(ES)
Kristi Laug
AFRL/PROP
1950 Fifth Street
Wright-Patterson AFB OH 45433
937-255-3362

10. SPONSOR/MONITOR'S ACRONYM(S)
N/A

11. SPONSOR/MONITOR'S REPORT NUMBER(S)
N/A

12. DISTRIBUTION / AVAILABILITY STATEMENT

Distribution Statement A: Approved for public release; distribution is unlimited.

13. SUPPLEMENTARY NOTES
N/A

14. ABSTRACT

15. SUBJECT TERMS

16. SECURITY CLASSIFICATION OF: UNCLASSIFIED			17. LIMITATION OF ABSTRACT	18. NUMBER OF PAGES	19a. NAME OF RESPONSIBLE PERSON
a. REPORT	b. ABSTRACT	c. THIS PAGE	Unlimited Distribution	See Attached List	Kristi Laug
					19b. TELEPHONE NUMBER (include area code) 937-255-3362

TITLE	AUTHORS	DATES	PAGES
The Place of Solar Thermal Rockets in space	C. C. Selph	May 81	24
Solar Thermal Propulsion from Concept to Reality	Karl J. Iliev	Aug 1996	11
Solar BI-Modal System Concept: Mission Applications, A Preliminary Assessment	Kristi K. Laug, Michael R. Holmes Kurt O. Westerman		5
Dual-Propulsion Technology Reusable Orbit Transfer Vehicle Study	Travis Elkins, Terence Galati		7
Studies of Hafnium-Carbide Wafers using a Thermogravimetric	Domingo G. Castillo, Paul F. Jones		11
One Dimensional Model of a Solar-Thermal Thruster Using a Porous Absorber/Heat Exchanger	Michael R. Holmes	October 15, 1993	29
Evaluation of Hafnium-Carbide Wafers for use in a Solar Calorimeter	Kristi K. Laug, Alan J. Baxter		7
Solar Thermal Propulsion Experiments Design	Kristi K. Laug	1996	11
Porous Disk Test Bed Report of Results	Richard Hurtz	Aug 10, 1990	24
The Solar Propulsion Concept is Alive and Well at the Astronautics Laboratory	Kristi K. Laug	Nov 26, 1993	70
Foam Inflated Rigidized Truss Structure Developed for an SRS Technologies Solar Concentrator	Dean M. Lester, David M. Cannon	1996	8
Fabrication of Thin Film Concentrators for Solar Thermal Propulsion Applications	Paul A. Cierow	1991	7
Scaling Characteristics of Inflatable Paraboloid Concentrators	Mitchell Thomas, Gordon Veal	1991	6
AFRPL Solar-Thermal Rocket Activities	C.C. Selph, G.J. Naujokas	March 1984	9
Dependence of Solar-Thermal Rocket Performance on Concentrator Performance	Michael R. Holmes, Kristi K. Laug	1995	12
A Comparison of the Performance of Seamed and unseamed Inflatable Concentrators	Arthur Palisoc, Mitchell Thomas	1995	10
Society for the Advancement of Material and Process Engineering	Thomas C. Walton, James V. Crivello		10
Ideal Performance of Off-Axis Paraboloid Concentrators for Solar Thermal Propulsion	Michael R. Holmes		7
A Performance Evaluation of an Inflatable Concentrator for Solar Thermal Propulsion	J.P. Paxton, M. R. Holmes		10
Prediction of the Response of a Polyimide Concentrator for Solar Thermal Propulsion	Paul A. Gierow, William R. Clayton, James D. Moore		8
Inflatable Concentrators for Solar Themal Proulsion	William R. Clayton, Paul A. Gierow	1992	6
The Long Term Storability and Expulsion ofRocket Propellants and Oxidizers	Gordon David Elder	Aug 13, 1987	5
Prediction of the Response of a PolyimideConcentrator forSolar Thermal Propulsion	Paul A. Gierow, James D. Moore		11
Conceptual Design Study of a Solar Concentrator	R. Prasinghe, Kristi K. Laug		13
PL (OLAC)/RKAS Concentrator Information	Michael R. Holmes	Feb 11, 1993	29
Dependence of Solar-Thermal Rocket Performance on Concentrator Performance	Michael R. Holmes, Kristi K. Laug	1995	12
Thruster Interface	Michael R. Holmes	May 4, 1994	23
Cumulative Power Plots	Kristi K. Laug		87

Solar Engineering – Vol. 2
ASME 1995

A COMPARISON OF THE PERFORMANCE OF SEAMED AND UNSEAMED INFLATABLE CONCENTRATORS

Arthur Palisoc and Mitchell Thomas
L'Garde, Inc.
Tustin, California

ABSTRACT

Tests were run comparing seamed and unseamed inflatable concentrators. Measurements of the surface profiles showed that the effect of seams on surface accuracy was minimal. Surface errors were generally slowly varying across the membrane, exhibiting a "W" or "M" shape. When the membrane included seams, the result was a slight bumpiness in the error profile which retained the "W" or "M" shape at nearly the same level as without seams. Recent studies indicated that the major source of the surface error was more likely the variation in material modulus as a function of position and stress. We used a special finite-element computer code to quantify the effect of seams; the results show again that the contribution of seams to the error in surface shape is negligible compared to the observed surface deviations in typical reflectors. The significance of these findings is that inflatable reflectors can be made inexpensively using seamed construction with no appreciable degradation of surface accuracy when compared to more expensive, continuous, formed membranes.

INTRODUCTION

NASA sponsored the building and testing of 3-m-diameter paraboloids in 1979. Figure 1 shows the shape of the deviation of a typical such paraboloid from the perfect paraboloid shape. This is the deviation for a scan about 670mm below the center of the symmetric 3-m-diameter inflated paraboloid. This reflector was made of many pie-shaped gores, seamed together, and the scan shown in Figure 1 crossed over a dozen or so such seams. If there are any slope discontinuities or error sources caused by scanning over the seams, they are insignificant compared to the obvious, systematic distortion. A gradual "W" shaped distortion is obtained from one side of the reflector to the other. This gradual distortion is typical of what is seen for these and other such reflectors built and measured [1,2].

During the NASA study, we postulated that the cause of the error seen is the change in the effective modulus of the film used caused by the presence of the seams. Since the seams are covered with a tape, they are thicker than the rest of the film. Since the relative density of tape is higher near the center of the reflector, where the pie-shaped gores are at their narrowest, the seams cause a systematic variation in effective modulus across the surface of the paraboloid. At the time this work was done, there did not exist accurate analysis tools that could prove the effects existed. In this paper we present some of the test data earlier obtained, and show supporting analyses recently performed using a new finite-element code designed for inflatable membranes (FAIM). The determination of the role of seams in surface accuracy is very important to quantify because construction of large paraboloids will most likely need to use seams. The alternatives are relatively expensive and have their own sets of problems. For instance, the modulus of the thin plastic films used for these reflectors varies considerably depending on how the film is manufactured. DuPont and other plastic film producers have spent much research and effort in developing methods for making rolls of flat film with relatively uniform modulus. A uniform modulus is necessary, especially for solar concentrators where the surface must be stretched smooth.

Off-the-shelf films such as Kapton have substantial space-flight experience. They can survive even in Low-Earth orbits when properly protected. On the Inflatable Torus Solar Array Technology Program, the Kapton substrate was protected from atomic oxygen attack and space charging by coating with Indium Tin Oxide - - a relatively inexpensive process.

HAIR TEST PROGRAM

A series of tests were run on Phase 1 of the Highly Accurate Inflatable Reflectors (HAIR) program in 1983 [3]. The analysis of the effect of seams on shape showed that there was a significant difference in the shape of gores once the seams were considered. Figure 2 shows the calculated gore edge dimensions (deviation from a straight line) for the cases of a uniform film and one with seams. The seam correction was made by taking a variable film thickness along the length of the gore corresponding to the extra thickness caused by the addition of the tape used on the seams. This variable thickness changes from a value nearlyequal to the sum of the triangular (pie-shaped) gore, to a value just slightly greater than the gore film alone at the broad end.

To test out this analysis a series of inflation tests were made on films. Table 1 shows the matrix of tests. For each type of specimen, a test was planned both with and without seams. The shape of the flat membranes when pressurized was given theoretically by [4]

$$d = d_{max}[1 - 0.887(r/a)^2 - 0.08674(r/a)^4 - 0.01884(r/a)^6] \quad (1)$$

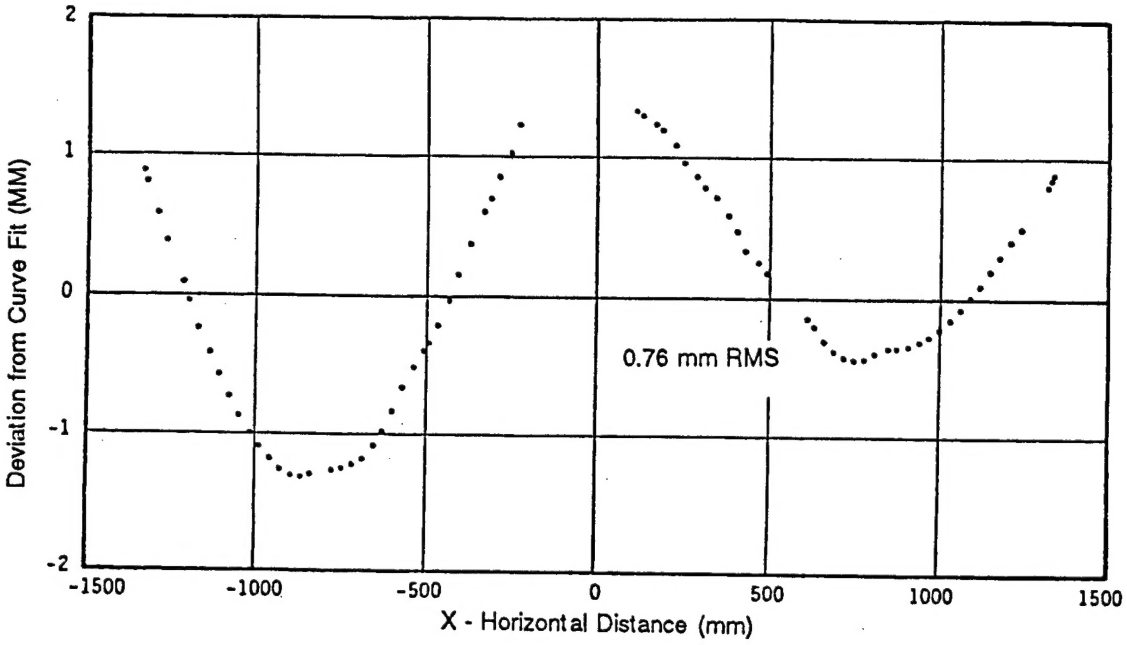

FIGURE 1. INACCURACY OF POLYESTER PARABOLOID (13 MPa FILM STRESS)

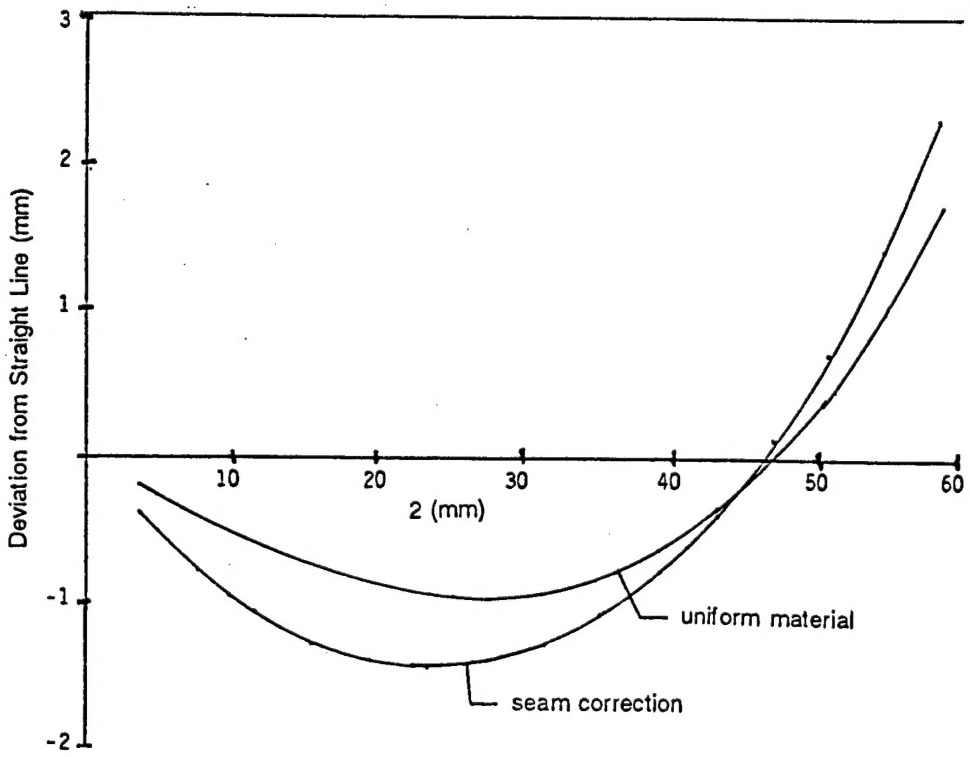

FIGURE 2. FLAT-PATTERN SHAPE FOR GORE OF PARABOLOID

TABLE 1. MATRIX OF INFLATABLE MEMBRANES TESTED AND REPORTED HERE

Thickness (Mils)	Seam Tape Thickness	Initial Shape	Mounting Method	Type of Specimen With Seams	Type of Specimen Without Seams	Design/Construction Method
0.25 0.25	1.0 0.5	For Paraboloid For Paraboloid	Stretched in place Stretched in place	X X		FLATE Code, no seams FLATE Code, with seams
0.25 0.25	None 0.5	Flat Flat	Flat Flat		X X	Flat Flat
1.0 1.0	None 1.0	Flat Flat	Flat Flat -		X X	Flat Flat
0.25	1.0	Flat	Flat	X		Seams stretched before taping, Eq. 1
0.25	0.5	Flat	Flat	X		Flat, lattice-work seams
1.0 1.0	None 1.0	Spherical (heat formed) Spherical (heat formed)	Unstretched Unstretched		X X	Assumed Flat Assumed Flat

where d is the deflection from the initial position, d_{max} is the deflection at the center of the film, a is the radius of the disk, and r is the radial distance from the center of the disk. The measured profiles of the inflated test specimens were compared to the theoretical ones (best fit) to get the shape of the deviation.

The inflated surface was measured using a laser mounted on an optical bench, and finding the positions of the spot reflected from the surface as a function of laser position (see [2]).

TEST RESULTS

Figure 3 shows a typical mounting of a test membrane on the face of vacuum chamber used to create the pressure difference for inflation. The test membranes were roughly 1 meter in diameter. Figure 4 shows the deviations found for two paraboloids - - using the two gore shapes shown in Figure 2. For the shape assuming a uniform material, we got the familiar "W" shaped curve found on the earlier NASA tests. For the paraboloid where a seam correction was assumed, the deviation reversed into a "M" shape. The implication is that if a proper correction factor can be found, somewhere in between these two cases, we should have a more accurate shape.

To check the hypothesis further, tests on flat membranes were run. Figures 5,6, and 7 show results for three flat membranes which were tested first without seams. Then, similar flat membranes were sliced into pie-shaped gores, seamed, and retested. The startling result was that in all three cases, there was little difference between the seamed and unseamed membranes. The effect of the seams could be seen in some of the membranes as small bumps riding on the main surface distortion. The major source of error in these membranes was clearly not the seams.

We explored this further with two additional specimens. First we examined a flat membrane that was then cut into a lattice (Figure 8) where seams were made running not only radially but also circumferentially. The measured surface deviations are shown in Figure 9; they look very similar to those measured earlier. We then formed a spherical membrane by heat-shrinking the mylar membrane over a mold. The resulting deviations from the theoretical shape is shown in Figure 10; they also have the familiar shape - - with little effect of seams.

Some later work has shown that the modulus of thin films typically varies strongly with strain [2]. Since paraboloids have varying radii of curvature, there is a systematic variation of strain as one travels from the center of a paraboloid to its edge. This variation in elastic modulus can be very large and may be the culprit causing the surface inaccuracies. The FAIM computer code discussed in the next section is currently being modified to include these effects.

These test data show that until we understand better the source of surface inaccuracies in inflated membranes, there is no increase in accuracy obtainable by going to unseamed membranes. Once we understand and control the sources of the deviations seen above, then perhaps research into unseamed membranes will provide even higher accuracy. The current state of the art, with deviations on the order of those seen above, will suffice for high quality solar concentrators (concentration ratios above 12,000) and microwave antennas (to mm-wavelengths).

Faim Description

In the late 1980's, L'Garde developed a finite element modeling program, FAIM (Finite Element Analysis of Inflatable Membranes), for the analysis of the large deformations of inflatable parabolic membranes. FAIM is a specialized, geometrically nonlinear finite

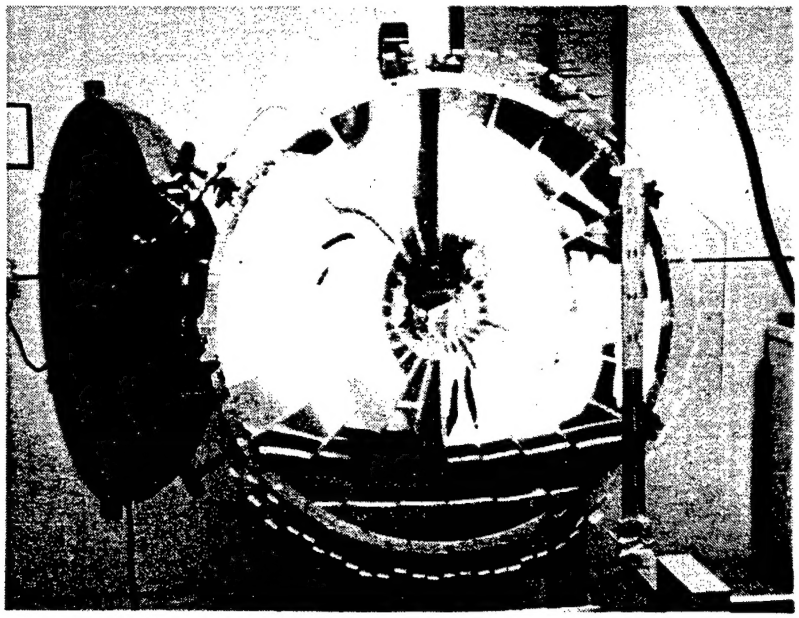

FIGURE 3. 24 GORE PARABOLOID

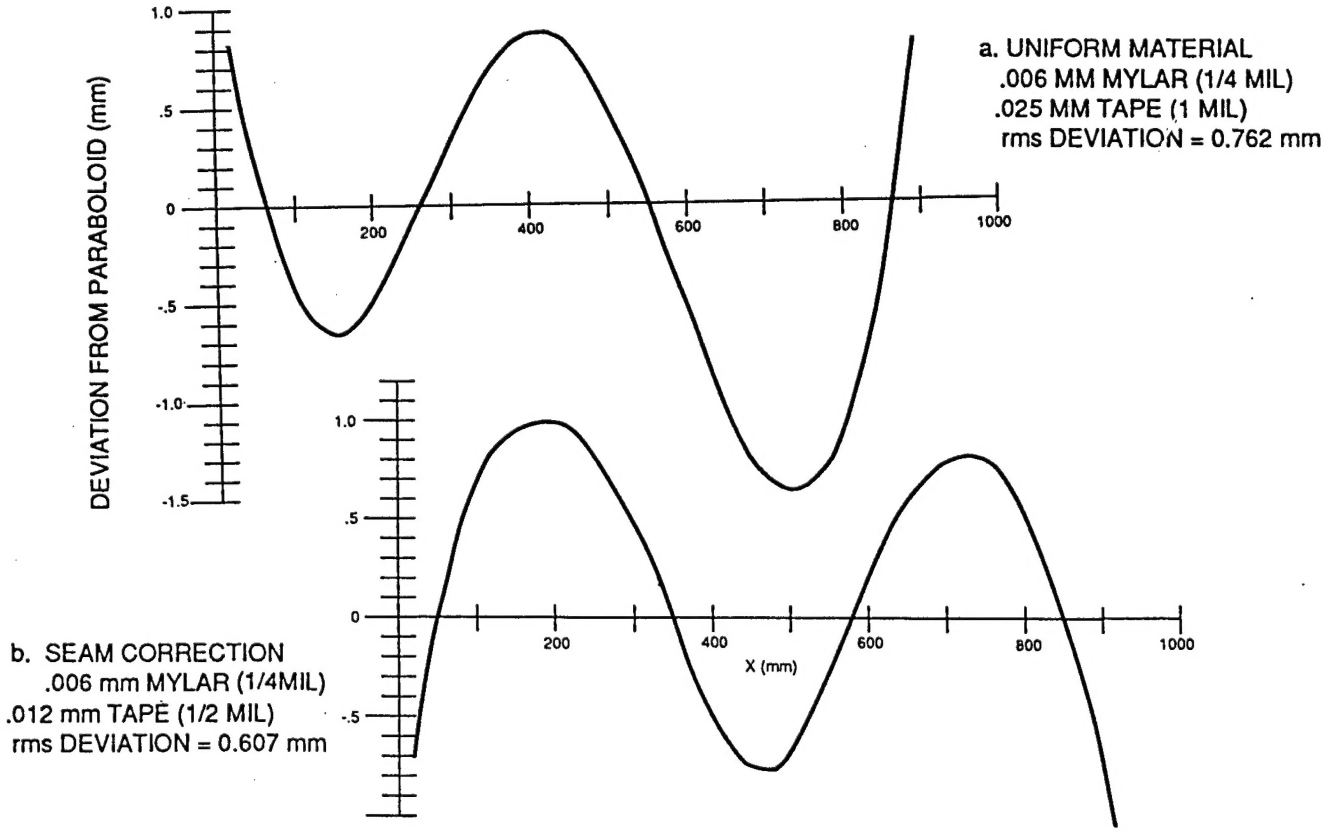

FIGURE 4. COMPARISON OF PARABOLOIDS USING TWO DIFFERENT FLAT PATTERNS

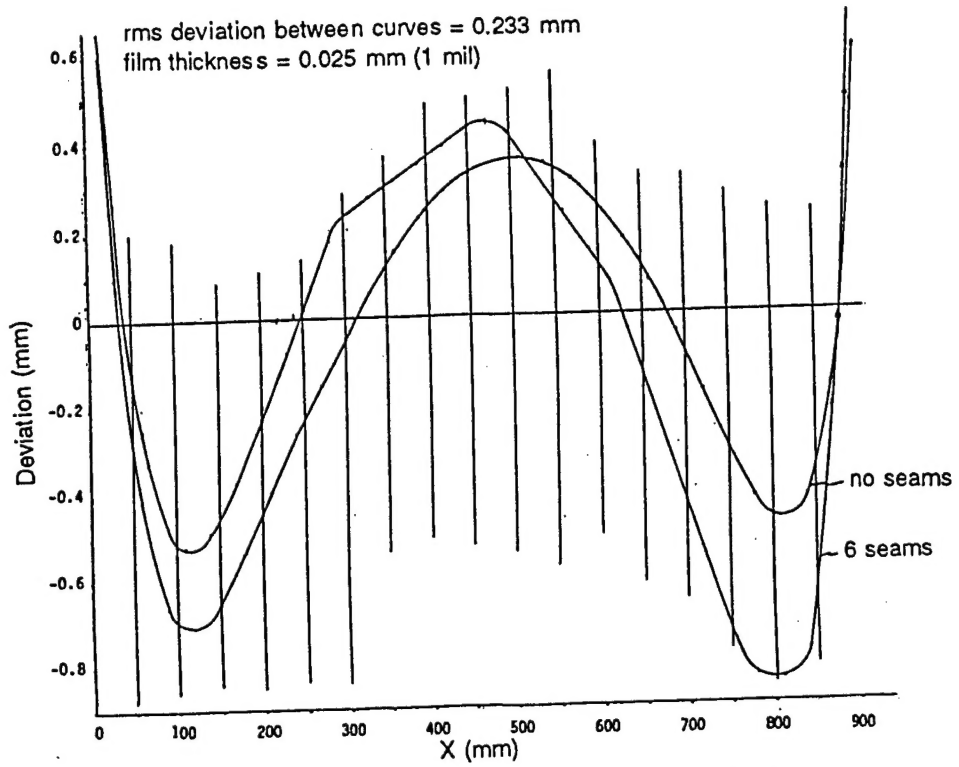

FIGURE 5. PERFORMANCE OF THIN, FLAT MEMBRANE

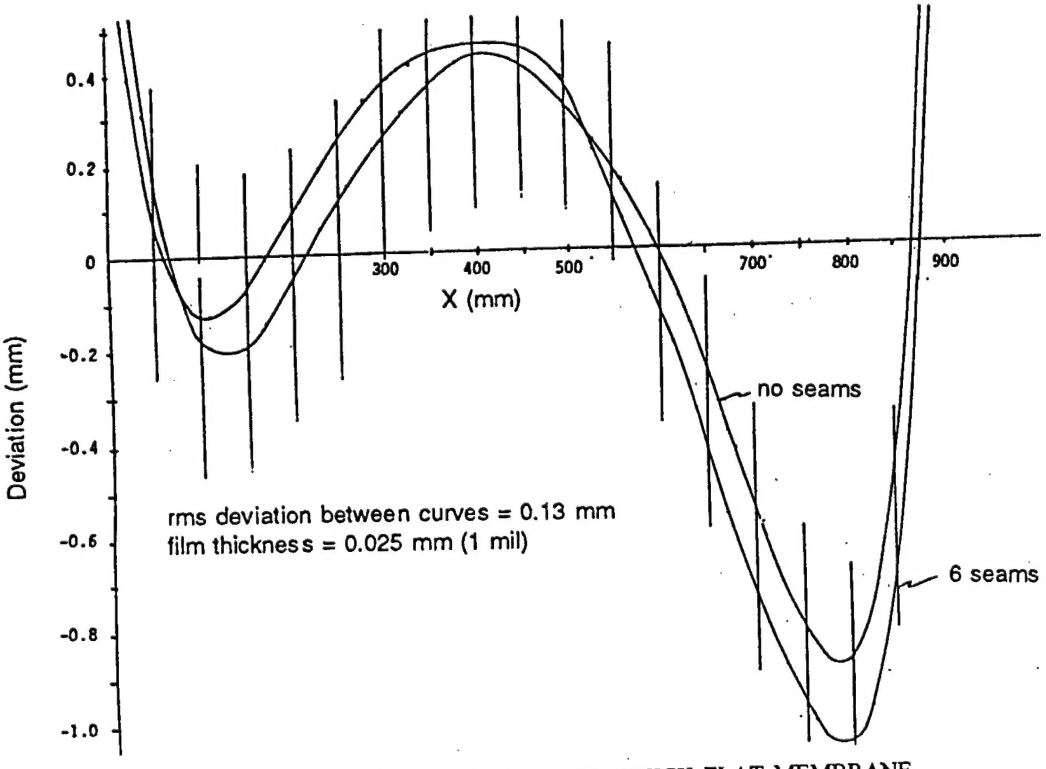

FIGURE 6. PERFORMANCE OF UNFORMED, THICK FLAT MEMBRANE

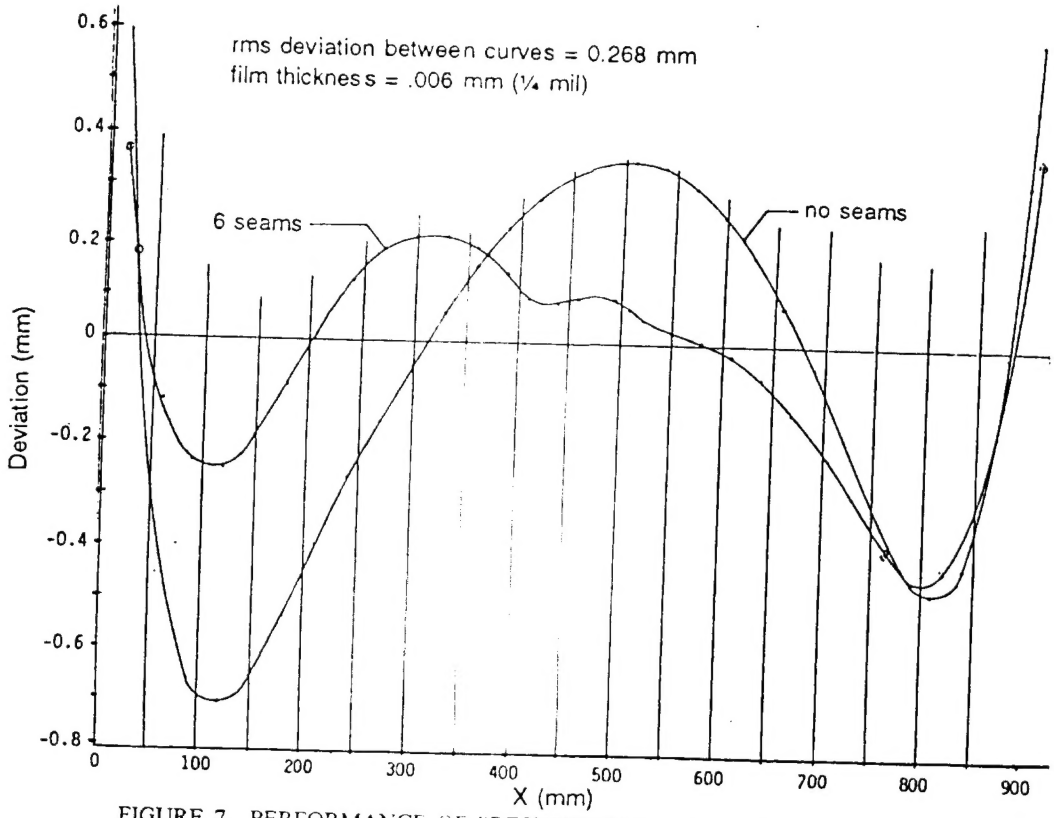

FIGURE 7. PERFORMANCE OF PRESTRETCHED, THIN, FLAT MEMBRANE

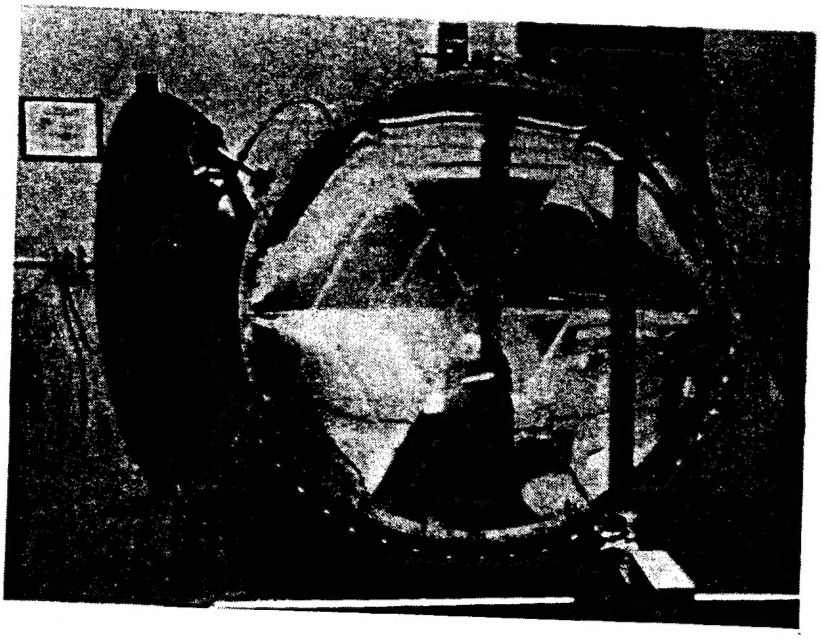

FIGURE 8. LATTICE-ENFORCED FLAT MEMBRANE

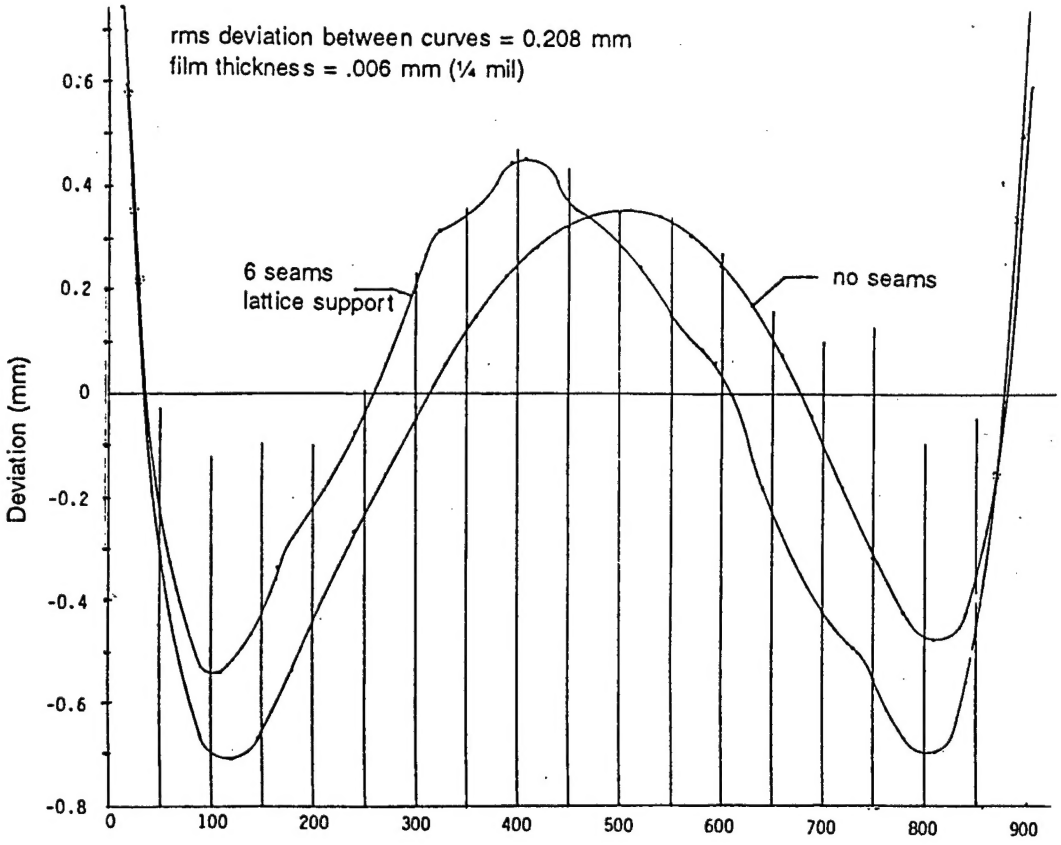

FIGURE 9. PERFORMANCE OF LATTICE-SUPPORTED, THIN, FLAT MEMBRANE

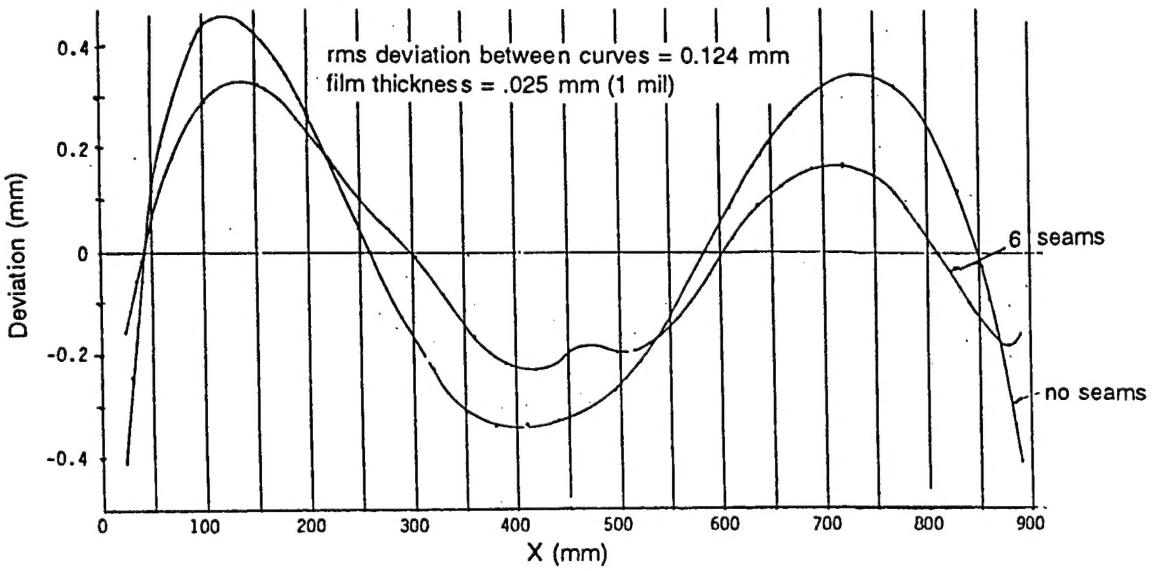

FIGURE 10. PERFORMANCE OF HEAT-FORMED, THICK, FLAT MEMBRANE

element program. It is iterative in nature; an initial prescribed, uninflated structural shape is input to be analyzed for stress and deformations.

In its current version, FAIM assumes a linear isotropic material and a geometrically nonlinear deformation behavior. The loadings available are (a) internal/external pressure, (b) concentrated nodal forces, and (c) nodal temperatures. Displacement, skew, and spring boundary conditions may be specified on any number of nodes of the finite element model. A number of enhancements have also been made to FAIM over the years in order to increase its analysis capabilities as well as its computational efficiency. First, a preprocessor and postprocessor with pull-down type menus were coded which makes the input and output interaction user-friendly. Secondly, two special analysis capabilities were implemented in the FAIM code in order to corroborate the stress and deformation behavior of inflatable parabolic shell membrane analytical models with their laboratory prototypes. A "spring boundary condition" mentioned above was coded in anticipation of the need to characterize the outer radius mounting surface of the parabolic shell as a flexible, rather than an infinitely rigid support. Also, a "prestress" capability was implemented in the code in order to characterize the prestress state of the gore membranes due to the mounting procedure. Currently, a node renumbering routine to reduce the bandwidth of the coefficient matrix is being written. This will reduce both the memory and CPU requirement of the code.

NASA has recently awarded L'Garde, Inc. a Phase II SBIR contract to incorporate nonlinear material and dynamics capability to FAIM. By the end of 1994, FAIM should have nonlinear material capability. And by the middle of 1995, the dynamics capability should be in place.

An 8-node isoparametric quad, a 6-node isoparametric triangle, and a 3-node isoparametric cable are the basic elements of the code. A conscious decision was made early to discard the computational advantage of the 4-node quadrilateral and the 3-node triangle membrane elements since these elements were deemed too crude to provide the requisite deformation information. A 3-node triangle for instance can only approximate the smooth surface of an inflatable parabolic shell surface with a collection of flat triangular facets. These facets, each of which has a constant slope are simply not adequate when one needs to determine the surface slopes throughout the continuum.

FAIM Validation Examples

FAIM was run on different computing platforms including a VAX, SUN, and PC486's using the Microsoft and Lahey FORTRAN compilers. Although the convergence process and the number of iterations varied from one computer to the next, the final result, once the convergence criterion has been satisfied, was the same for all computers and compilers within the specified tolerance.

The very first validation test FAIM was subjected to was the large deflection of a seamless paraboloid. For this test, one of the authors (M.T.) solved analytically, the inverse problem of calculating the initial uninflated shape of a surface of revolution so that on inflation to the design pressure, the surface takes on a prescribed paraboloidal shape. [5] The uninflated shape was input to FAIM, and the same internal pressure applied to see if FAIM gives back the correct inflated shape. The results of FAIM against the analytical solution are shown in Figure 11. Figure 11 shows the results for three different initial uninflated shapes corresponding to three values of the Poisson ratio. For the case shown, the edge of the paraboloid was fixed.

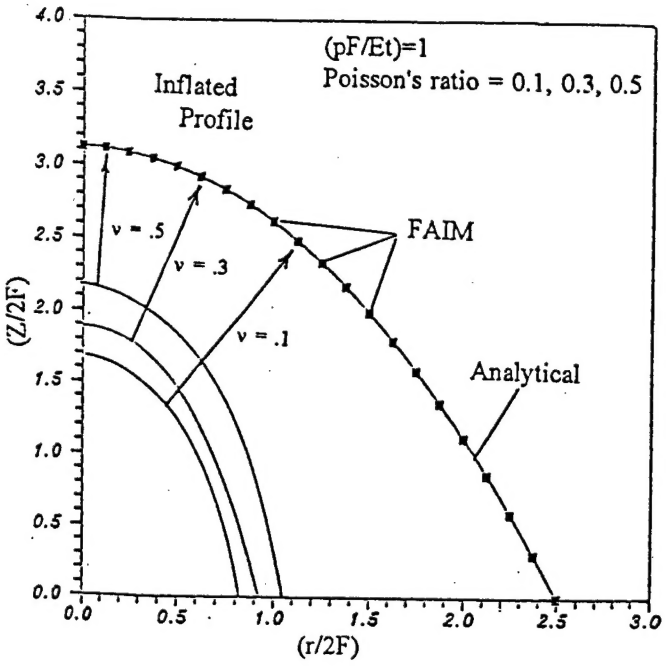

FIGURE 11. LARGE DEFLECTION (pF/Et=1) OF INFLATABLE PARABOLOID

In the figure, r is the radius $r^2 = x^2 + y^2$ in the paraboloid equation $z = (1/4F)r^2$. F is the focus of the paraboloid, E is the material modulus, p is the inflation pressure, and t is the material thickness.

One other test used was that of the deflections of a circular membrane. [6] Excellent agreement was found between the analytical solutions and FAIM-calculated results. The result for the deformation of an initially flat circular membrane, clamped at the edge is shown in Figure 12.

The Effect of Seams on RMS Surface Accuracy

In order to assess the effect of seamed-construction on the rms surface accuracy of inflatables, 3 cases with and without seams were examined: (i) the deflection of a one-meter diameter six-gore, flat circular membrane, (ii) the deflection of a one-meter six-gore, pre-formed spherical membrane, and (iii) the deflection of an axisymmetric 64-gore, 14-meter diameter on-axis parabolic reflector.

The resulting deflections for the flat membranes, cases (i) and (ii) above were fitted to the equation describing the shape of a pressurized membrane constrained at a circumference (see eq. 1). For the cases considered in this section, we used the form

$$z = P_1 + P_2(x^2 + y^2) + P_3(x^2 + y^2)^2 \qquad (2)$$

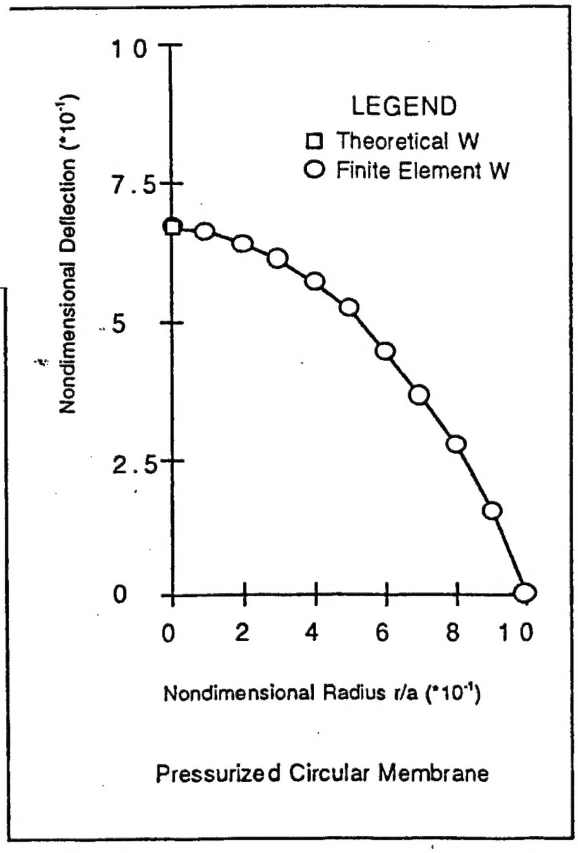

FIGURE 12. DEFLECTION OF PRESSURIZED CIRCULAR MEMBRANE

The finite element model for the circular membranes is shown in Figure 13. The preformed membrane is taken from a sphere of 95 inch radius (Figure 14).

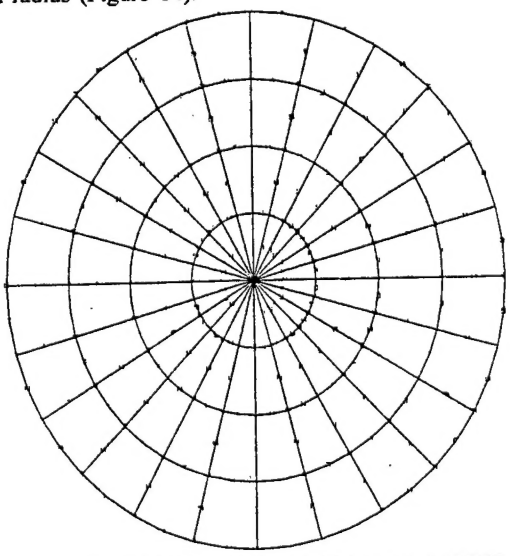

FIGURE 13. FINITE ELEMENT MODEL OF CIRCULAR MEMBRANE

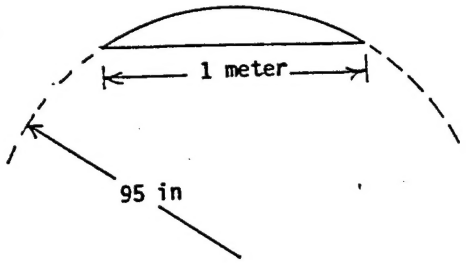

FIGURE 14. PREFORMED SPHERICAL MEMBRANE FROM 95 INCH RADIUS SPHERE

Table 2 shows the results of the finite element calculation. In the seamed cases, the gores are joined together using a 3/8 inch wide 0.5 mil thick tape.

TABLE 2a. PARAMETERS OF EQ.(2) FOR FLAT CIRCULAR MEMBRANE

	Without Cable	With Cable (Seams)
P_1(in)	2.8905	2.8397
P_2(in^{-1})	-0.00627	-0.00602
P_3(in^{-3})	-3.04871 x 10^{-6}	-3.6452 x 10^{-6}
Sum of Squares	0.00339 in^2	0.00617 in^2
rms Deviation	0.00342 in	0.00462 in

TABLE 2b. PARAMETERS OF EQ.(2) FOR PREFORMED MEMBRANE

	Without Cable	With Cable (Seams)
P_1(in)	95.75858	95.71093
P_2(in^{-1})	-0.00734	-0.00708
P_3(in^{-3})	-3.65680 x 10^{-6}	-4.03734 x 10^{-6}
Sum of Squares	0.00544 in^2	0.00784 in^2
rms Deviation	0.00434 in	0.00521 in

The results listed in Table 2 show that the change in rms surface accuracy relative to the membrane surface shape is very small. As expected, the cable provides some "stiffening" as shown by P_1, but

the rms surface accuracy relative to the overall profile remains about the same. Moreover, when L'Garde designs its reflectors using flat gores, the effect of the thicker seams is taken into consideration so that the final inflated shape of the surface is parabolic.

The next case shown in Table. 3 is that of a 64-gore, 14-meter diameter on-axis inflatable parabolic reflector. The *F/d* ratio is *1.0* and the material used is *0.25* mil-thick, with a modulus of *E=550,000* psi, and a Poisson ratio of 0.3. The surface was fitted to the following equation:

$$z = z_o + A^*((x-x_o)^2 + (y-y_o)^2) \quad (3)$$

where

$$A = (1/4F) \quad (4)$$

TABLE 3. PARAMETERS OF EQ. (3) FOR THE 14-METER DIAMETER REFLECTOR

	With Seams
A	4.58684×10^{-6}
X_o	5.43186 in
Y_o	0.28831 in
Z_o	0.28393 in
rms Deviation	0.00433 in (0.11 mm)

In Table 3 we show only the case with cables (seams) since we have already seen that FAIM predicts to a high degree of accuracy the final inflated shape even of a highly deformed seamless membrane (See Figure 11). The table lists the parameters of Eq. (3) including the rms surface accuracy. As was mentioned earlier, the initial uninflated flat gores used were shaped taking into account the effect of the thicker seams. We see from the table that the rms surface accuracy predicted by FAIM is 0.11 mm rms. This is about an order of magnitude lower error than that measured for large inflatable reflectors. Seams are not causing the observed larger deviations.

CONCLUSIONS

Tests of inflated membranes have shown that the presence of seams causes surface errors of about 0.1 mm rms in 1-meter diameter membranes. On top of this rides a systematic error which is about an order of magnitude greater. Theoretical calculations using finite element analysis confirms that the presence of seams can not explain the observed surface errors; these calculations show that the seam effect should be less than 0.1 mm rms error. Seams can be included in membrane design using a variable thickness of the membrane corresponding to the average thickness including the seam tape.

The advantage of the seamed construction is that large membranes can be made inexpensively, using off-the-shelf films that are relatively well characterized. Seamed construction is currently feasible for inflatable reflectors for microwave antennas to 5 GHz and for optical concentrators for concentration ratios up to 12,000. When the systematic error found in inflated membranes is characterized and removed, these limits may be extended considerably before seams significantly affect the results.

ACKNOWLEDGMENTS

The testing of inflated membranes was sponsored by NASA and the USAF, and was carried out under the direction of Gordon Veal of L'Garde. The FAIM computer code was developed by L'Garde, with some assistance from NASA. The FAIM calculations reported here were sponsored by L'Garde.

REFERENCES

1. G.J. Friese, G. D. Bilyeu, and M. Thomas, "Initial '80's Development of Inflated Antennas," L'Garde Report LTR-82-GF-107, NASA Contractor's Report, December 1982.

2. Mitchell Thomas and Gordon Veal, "Scaling Characteristics of Inflatable Paraboloid Concentrators," Solar Engineering, ASME Book No. H00630, 1991.

3. M. Thomas and G. Veal, "Highly Accurate Inflatable Reflectors," Report AFRPL TR-84-021, May 1984. (AD-A143628)

4. H. Hencky, "Über den Spannungszustand in kreisrunden Platten mit verschwindender Biegungssteifigkeit," Zeits. Math. Phys., Vol. 63, 311-316 (1915), (with some numerical corrections).

5. G. R. Veal, "Highly Accurate Inflatable Reflectors, Phase II," Report AFRPL TR-86-089, March 1987 (AD-B111435).

6. A. Palisoc, "A User Interface and Finite Element Analysis of Inflatable Off-Axis Parabolic Antennas," L'Garde Technical Report LTR-93-AP-043, July 1993.